

Electroweak multi-Higgs production: A smoking gun for the Type-I 2HDM

Tanmoy Mondal,^{1,*} Stefano Moretti,^{2,3,†} Shoaib Munir,^{4,‡} and Prasenjit Sanyal^{5,§}

¹*Department of Physics, Osaka University, Toyonaka, Osaka 560-0043, Japan*

²*School of Physics & Astronomy, University of Southampton, Southampton SO17 1BJ, UK*

³*Department of Physics & Astronomy, Uppsala University, Box 516, SE-751 20 Uppsala, Sweden*

⁴*East African Institute for Fundamental Research (ICTP-EAIFR), University of Rwanda, Kigali, Rwanda*

⁵*Department of Physics, Konkuk University, Seoul 05029, Republic of Korea*

(Dated: April 18, 2023)

Extending the Higgs sector of the Standard Model (SM) by just one additional Higgs doublet field leads to the 2-Higgs Doublet Model (2HDM). In the Type-I Z_2 -symmetric limit of the 2HDM, all the five new physical Higgs states can be fairly light, $\mathcal{O}(100)$ GeV or less, without being in conflict with current data from the direct Higgs boson searches and the B -physics measurements. In this article, we establish that the new neutral as well charged Higgs bosons in this model can all be simultaneously observable in the multi- b final state. The statistical significance of the signature for each of these Higgs states, resulting from the electro-weak (EW) production of their pairs, can exceed 5σ at the 13 TeV High-Luminosity Large Hadron Collider (HL-LHC). Since the parameter space configurations where this is achievable are precluded in the other, more extensively pursued, 2HDM Types, an experimental validation of our findings would be a clear indication that the true underlying Higgs sector in nature is the Type-I 2HDM.

Keywords: Higgs boson, Scalar, LHC, 2HDM

I. INTRODUCTION

The existence of additional Higgs bosons, besides the one discovered by the LHC [1, 2] (hereafter, denoted by H_{obs}), is predicted by most (if not all) frameworks of new physics. Observation of a second Higgs boson will thus provide firm evidence that the underlying manifestation of the EW Symmetry Breaking (EWSB) mechanism is a non-minimal one.

From a theoretical point of view, given the fact that the H_{obs} belongs to a complex doublet field in the SM, any additional Higgs field can be naturally expected to have the same $SU(2)_L$ representation. Following this argument, even the minimal bottom-up approach of augmenting the SM with a second doublet Higgs field and assuming CP-invariance yields a total of five physical Higgs states after EWSB: two neutral scalars (h and H , with $m_h < m_H$), one pseudoscalar (A), and a charged pair (H^\pm). If both the doublets Φ_1 and Φ_2 in this 2HDM couple to all the fermions of the SM, they would cause flavor-changing neutral currents (FCNCs) that contradict the experimental results. To prevent these FCNCs, a Z_2 symmetry can be imposed [3, 4], under which $\Phi_1 \rightarrow \Phi_1$, $\Phi_2 \rightarrow -\Phi_2$, $u_R^i \rightarrow -u_R^i$, $d_R^i \rightarrow -d_R^i$, $e_R^i \rightarrow -e_R^i$, so that all the quarks and charged leptons (conventionally) couple only to the Φ_2 , resulting in the so-called Type-I 2HDM (see [5, 6] for detailed reviews).

By now, many studies [7–24] have established that the additional Higgs states (when the H_{obs} is identified with either the h or the H state) of the 2HDM can

be individually accessed at the LHC. Therefore, several searches for singly-produced neutral and charged Higgs bosons have been carried out by the ATLAS and CMS collaborations (see, e.g., [25–32]), but they remain elusive thus far. Even if a single state is eventually observed, the corresponding measurements that will ensue will, however, not enable one to ascertain which of the many possible extended realisations of the Higgs mechanism is at work. For an unequivocal extraction of the complete EWSB dynamics, it is imperative that all the various components of the scalar potential be accessed experimentally. This makes the study of multi-Higgs final states mandatory.

The majority of analyses, both phenomenological and experimental ones, involving an electrically neutral multi-Higgs final state, concentrate on QCD-induced production modes, namely, gluon-fusion and $b\bar{b}$ -annihilation (where the b -quarks are themselves actually produced from a (double) gluon splitting). While such gluon-initiated (multi-)Higgs production is evidently highly dominant in the SM, it is not necessarily so in new physics models, owing to the non-standard couplings of their new Higgs bosons to the fermions and gauge bosons. In a previous analysis [33] it was shown that the inclusive cross sections for the $q\bar{q}^{(\prime)}$ -induced production, where q represents predominantly a valence (u or d) quark, of neutral multi-Higgs final states can be larger than their QCD-induced production, over sizeable parameter space regions of the Type-I 2HDM with standard hierarchy ($H_{\text{obs}} \equiv h$). The charged final states can of course only be produced via EW processes.

In this article, through a complete detector-level Monte Carlo (MC) analysis, we concretely establish that EW production can provide simultaneously visible signals of all the three additional Higgs bosons of the Type-I 2HDM at the LHC with 3000 fb^{-1} integrated luminos-

* tanmoy@het.phys.sci.osaka-u.ac.jp

† s.moretti@soton.ac.uk; stefano.moretti@physics.uu.se

‡ smunir@eaifr.org

§ prasenjit.sanyal01@gmail.com

ity. The model parameter space configurations where this is possible contain an A lighter than the H_{obs} , with the H and H^\pm not much heavier, and are therefore well-motivated, in that the entire Higgs spectrum lies at the EW scale. Our signature channel, constituting of multiple b -quarks, allows a full reconstruction of the H , A and H^\pm masses (with the h already observed elsewhere). It implies that the LHC can uniquely pin down (or definitively rule out) the underlying EWSB mechanism as this (albeit narrow) parameter space region of the Type-I 2HDM (or at least as a low-energy manifestation of a grander framework with a Higgs sector mimicking this model). What makes our results all the more significant is the fact that such a particular Higgs boson mass spectrum is forbidden in the Type-II 2HDM [34] (the realisation preferred by minimal Supersymmetry).

The article is organised as follows. In Sec. II we very briefly review the Type-I 2HDM, its parameter space configurations relevant for multi-Higgs production and the corresponding benchmark points (BPs) satisfying the most important theoretical and experimental constraints. In Sec. III we detail our MC analysis, and in Sec. IV we establish the sensitivity of the LHC to our multi-Higgs states and its ability to extract all the Higgs boson masses in the model. We present our conclusions in Sec. V.

II. THE TYPE-I 2HDM

A. Higgs potential and parameters

The most general potential of a CP-conserving 2HDM can be written as

$$\begin{aligned} \mathcal{V} = & m_{11}^2 \Phi_1^\dagger \Phi_1 + m_{22}^2 \Phi_2^\dagger \Phi_2 - [m_{12}^2 \Phi_1^\dagger \Phi_2 + \text{h.c.}] \\ & + \frac{\lambda_1}{2} (\Phi_1^\dagger \Phi_1)^2 + \frac{\lambda_2}{2} (\Phi_2^\dagger \Phi_2)^2 + \lambda_3 (\Phi_1^\dagger \Phi_1) (\Phi_2^\dagger \Phi_2) \\ & + \lambda_4 (\Phi_1^\dagger \Phi_2) (\Phi_2^\dagger \Phi_1) + \left[\frac{\lambda_5}{2} (\Phi_1^\dagger \Phi_2)^2 + \text{h.c.} \right]. \end{aligned} \quad (1)$$

It is convenient to write the doublets Φ_1 and Φ_2 , after EWSB, in terms of their respective vacuum expectation values (VEVs) v_1 and v_2 , the Goldstone bosons G and G^\pm and the physical Higgs states as

$$\begin{aligned} \Phi_1 = & \frac{1}{\sqrt{2}} \begin{pmatrix} \sqrt{2} (G^+ c_\beta - H^+ s_\beta) \\ v_1 - h s_\alpha + H c_\alpha + i (G c_\beta - A s_\beta) \end{pmatrix}, \\ \Phi_2 = & \frac{1}{\sqrt{2}} \begin{pmatrix} \sqrt{2} (G^+ s_\beta + H^+ c_\beta) \\ v_2 + h c_\alpha + H s_\alpha + i (G s_\beta + A c_\beta) \end{pmatrix}, \end{aligned} \quad (2)$$

where $\beta \equiv \tan^{-1}(v_1/v_2)$ and α are the angles rotating the CP-odd and the CP-even interaction states, respectively, into physical Higgs states, with s_x (c_x) implying $\sin(x)$ ($\cos(x)$). Using the tadpole conditions of the \mathcal{V} , m_{11}^2 and m_{22}^2 can be replaced by v_1 and v_2 (and subsequently by t_β – short for $\tan \beta$ – and $v \equiv \sqrt{v_1^2 + v_2^2} = 246$ GeV) as the free parameters of the model. Furthermore, the physical Higgs boson masses and the parameter $s_{\beta-\alpha}$ can be traded in for λ_{1-5} .

B. Multi- A production and benchmark scenarios

The benefit of using the physical Higgs boson masses as input parameters is that we can fix $m_h = 125$ GeV, so that our analysis corresponds to the ‘standard hierarchy’ scenario with $h = H_{\text{obs}}$ and a heavier H . For this scenario, our previous study [33] found that not only can the cross section for the EW production of the HA pair be up to two orders of magnitude larger than the gg/bb -induced one, but it also remains quite substantial for the subsequent states AAA and AAZ . Evidently, this cross section is more pronounced in parameter space regions where the H is produced on-shell, with a mass just above the AA or AZ decay threshold and a maximal corresponding branching ratio (BR). The $\text{BR}(H \rightarrow AA)$ can be enhanced if the $H \rightarrow hh$ decay is not kinematically allowed. The requirement of the couplings of the h to be SM-like, as is the case for the H_{obs} , pushes the model into the so-called alignment limit, where $s_{\beta-\alpha} \rightarrow 1$ [35]. In this limit, the HAZ coupling, which is proportional to $s_{\beta-\alpha}$, and hence the $\text{BR}(H \rightarrow AZ)$ is also naturally enhanced, while the $H \rightarrow hh$ and $H \rightarrow VV$ decays, even when available, are suppressed.

In light of the above observations, our analysis pertains to small, ~ 50 GeV, values of m_A . For such a light A , $b\bar{b}$ is by far the dominant decay mode and the multi-Higgs states that we are interested in here are thus the ones yielding at least 4 b -quarks via intermediate A s. Such states result from the EW production of either a neutral pair of Higgs bosons, both on-shell, as

$$\begin{aligned} AAA : & q\bar{q} \rightarrow H(\rightarrow AA)A \rightarrow 4b + X, \\ AAZ : & q\bar{q} \rightarrow H(\rightarrow AZ)A \rightarrow 4b + X, \\ AAWW : & q\bar{q} \rightarrow H^+(\rightarrow AW)H^-(\rightarrow AW) \rightarrow 4b + X, \end{aligned}$$

or a charged pair, as

$$\begin{aligned} AAW : & q\bar{q}' \rightarrow H^\pm(\rightarrow AW)A \rightarrow 4b + X, \\ AAAW : & q\bar{q}' \rightarrow H^\pm(H^\pm \rightarrow AW)H(\rightarrow AA) \rightarrow 4b + X, \\ AAZW : & q\bar{q}' \rightarrow H^\pm(H^\pm \rightarrow AW)H(\rightarrow AZ) \rightarrow 4b + X. \end{aligned}$$

Here the W and Z decay inclusively (i.e., both hadronically and leptonically) and X can thus be any additional quarks (including b -quarks) and/or leptons.

In order to find configurations with substantial EW production cross sections, we fixed m_A to two representative values of 50 GeV and 70 GeV, and numerically scanned the remaining free parameters in the ranges

$$\begin{aligned} m_H : & [2m_A - 250] \text{ GeV}, \quad m_{H^\pm} : [100 - 300] \text{ GeV}, \\ s_{\beta-\alpha} : & 0.9 - 1.0, \quad m_{12}^2 : 0 - m_A^2 \sin \beta \cos \beta, \quad t_\beta : 1 - 60, \end{aligned}$$

using the 2HDMC code [36]. In these scans, the condition for the oblique parameters S , T and U to fall within the 95% confidence level (CL) ellipsoid based on the 2022 PDG values [37], $S = -0.01 \pm 0.07$ and $T = 0.04 \pm 0.06$, with correlations $\rho_{ST} = 0.92$ for $U = 0$, forced the mass of H^\pm to lie close to m_H . The theoretical predictions of these observables are also computed

BP	m_A	m_{H^\pm}	m_H	t_β	$s_{\beta-\alpha}$	m_{12}^2	BR(AA)	BR(AZ)
1	70	169.7	144.7	7.47	0.99	2355	0.99	0.006
2	50	169.8	150.0	17.1	0.98	1275	0.48	0.505

TABLE I. Input parameter values and BRs of the H for the two selected BPs. All masses are in GeV.

by 2HDMC. The B -physics observables, $\text{BR}(B \rightarrow X_s \gamma)$, $\text{BR}(B_u \rightarrow \tau^\pm \nu_\tau)$ and $\text{BR}(B_s \rightarrow \mu^+ \mu^-)$ were computed by the public code SuperIso v4.1 [38] and were required to meet the constraints on the $m_{H^\pm} - t_\beta$ plane derived in [34, 39] based on experimental results.

We extracted two BPs from the successfully scanned parameter space points. For BP1, with $m_A = 70$ GeV, the AA decay of the H is by far dominant over its AZ decay. Further, BP2 corresponds to $m_A = 50$ GeV and is selected to demonstrate the efficiency of our reconstruction method for the case when the $H \rightarrow AZ$ decay is also substantial, as noted in the last two columns of Table I. We point out here that all the Higgs states in both these BPs satisfy the 95% CL constraints included in the program HiggsBounds 5.10.2 [40], while the couplings of h to the SM are consistent with the combined 1σ measurements for H_{obs} from the ATLAS and CMS collaborations [41].

III. SIGNAL ISOLATION

The background events for the multi- b final states that we consider here originate predominantly from the QCD multi-jet and $t\bar{t}$ + jets processes. In our computation, we matched the multi-jet background up to four jets and the $t\bar{t}$ up to two jets. Our matched cross section for the multi-jet background in the 5-flavour scheme at the LHC with $\sqrt{s} = 13$ TeV is 8.98×10^6 pb, with nn231o1 [42] Parton Distribution Functions (PDFs) and a matching scale of 67.5 GeV. The $t\bar{t}$ production cross section is 833.9 pb, as calculated with the Top++2.0 [43] program, assuming a top quark mass of 173.2 GeV. For our simulation we generated 10^8 multi-jet events and 10^7 $t\bar{t}$ events. Other possible background processes include $t\bar{t}b\bar{b}$, $t\bar{t} + V$ (where $V = Z/W$), $V + \text{jets}$, ZZ and hZ , but we found them to be negligible after the selections.

For the two selected BPs, we used the NNPDF_LO_118 PDF set to estimate the multi- b signal events. The cross sections corresponding to the various signal modes, assuming an next-to-next-to-leading order k -factor of 1.35 [44], are given in Table II. We performed event-generation and parton shower with MadGraph5_aMC@NLO [45, 46] and Pythia 8 [47, 48], using the anti- k_t algorithm [49] for jet-reconstruction and b -tagging [50], with the default (mis-)tagging efficiencies as in the CMS tcl card [50]. This was then followed by event-reconstruction and analysis using Delphes [51] and Root [52]. The primary selection cuts we applied for signal isolation include: $p_T > 20$ GeV, $|\eta| < 5$ for all jets, separation $\Delta R = 0.4$ for any recon-

BP	σ_{AAA}	σ_{AAZ}	σ_{AAW}	σ_{AAW}	σ_{AAA}	σ_{AAZ}
1	199.8	0.88	31.6	165.7	96.9	0.43
2	117.3	91.8	34.8	228.2	45.1	35.3

TABLE II. Cross sections (in fb) in each of the signal channels considered here for the two selected BPs.

structed object, and $\cancel{E}_T > 10$ GeV. Further selections that we made for each Higgs state are explained below.

A. Reconstruction of the A

1. Since all the signal processes contain at least two A s, the events should contain at least 4 b -jets, a, b, c and d , which can be resolved into pairs 1 and 2. For this purpose we used a jet-pairing algorithm to choose one combination out of the possible three: $(a, b; c, d)$, $(a, c; b, d)$, and $(a, d; b, c)$, which minimizes [53]

$$\Delta R = |(\Delta R_1 - 0.8) + (\Delta R_2 - 0.8)|, \quad (3)$$

where, for a given combination,

$$\begin{aligned} \Delta R_1 &= \sqrt{(\eta_a - \eta_b)^2 + (\phi_a - \phi_b)^2}, \\ \Delta R_2 &= \sqrt{(\eta_c - \eta_d)^2 + (\phi_c - \phi_d)^2}. \end{aligned} \quad (4)$$

This algorithm is motivated by the idea that the b -jets coming from a resonance (presumably the A) would be closer together compared to uncorrelated ones.

2. After the pairing, we imposed an asymmetry cut,

$$\bar{\alpha} = \frac{|m_1 - m_2|}{m_1 + m_2} < 0.2, \quad (5)$$

where m_1 and m_2 are the invariant masses of the two b -jet pairs. This cut ensures that these two pairs are from identical resonances, i.e., from AA .

B. Reconstruction of the H^\pm

1. All events should contain at least 4 b -tagged jets and a pair of leading jets (thus corresponding to the dominant $q\bar{q}' \rightarrow A_1 H^\pm \rightarrow A_1 A_2 W^\pm \rightarrow 4b + jj$ process).
2. The invariant mass of the leading jj should lie within the $m_W \pm 25$ GeV mass window.
3. The four b -jets were combined into two b -jet pairs and only events where the invariant mass of each of these pairs lied within a 45 GeV window around m_A and satisfied the asymmetry cut $\bar{\alpha} < 0.2$ were selected. This criterion reduces the background significantly. The vector p_T -sum of the b -jet pairs estimated the p_T of the reconstructed A s, which are identified as A_1 and A_2 such that $p_T(A_1) > p_T(A_2)$ (since A_2 originates from the decay of the H^\pm and is softer).

4. When more than one pairings of the b -jets satisfies the above condition, we selected the combination which maximised the separation $\Delta R = \sqrt{(\Delta\eta)^2 + (\Delta\phi)^2}$ of the reconstructed H^\pm and A_1 .
5. We calculated the invariant mass of the $2b + jj$ system, where ‘ $2b$ ’ is the softer pair (identified as the A_2), to obtain the m_{H^\pm} .

C. Reconstruction of the H

1. The dominant signal process is $q\bar{q} \rightarrow A_1 H \rightarrow A_1 A_2 A_3 \rightarrow 4b + X$, so each event should contain at least six b -tagged jets. We combined these into three b -jet pairs and selected the combination for which the invariant mass of each pair lied within the m_A window and also satisfied the $\bar{\alpha}$ -cut.¹
2. The p_T of each b -jet pair was obtained by summing the 4-momenta of the two b -jets in it. Out of the three pairs, we identified the one with the highest p_T as the prompt A_1 . The remaining system of 4 b -jets then corresponded to the $A_2 A_3$ pair from H decay, and its invariant mass thus reconstructed the m_H .
3. As in the case of the H^\pm , if multiple pairings of the b -jets satisfied the above criteria, we used that 4 b -jet system for reconstructing the H which maximized its separation from the third b -jet pair (i.e., the prompt A_1) in the $\eta - \phi$ space.
4. Since tagging 6 b -jets is highly challenging due to finite (mis-)tagging, events with at least 5 b -jets were also used for reconstructing the H . In this case, the light jet with the leading p_T was first assumed to be the 6th b -jet for performing steps 1 – 3. If this jet failed to satisfy the pairing criteria above, these steps were repeated sequentially for the jet with the next highest p_T , until the correct jet was found.

IV. SIGNIFICANCES AT THE LHC

Using the steps detailed in the previous section, we calculated the signal (background) event rates, S (B) assuming an integrated luminosity of 3000 fb^{-1} at the LHC. In Fig. 1 we show the normalized invariant mass distributions of the b -jet pairs for the BP1 signal and background events. The subscript a implies the distribution for the pair containing the leading b -jet. The signal distributions in this figure as well as the subsequent

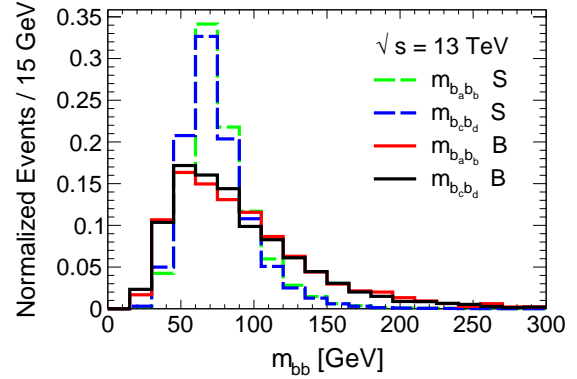


FIG. 1. m_{bb} distributions for the signal (green/blue - dashed) and background (black/red - solid) events for the BP1.

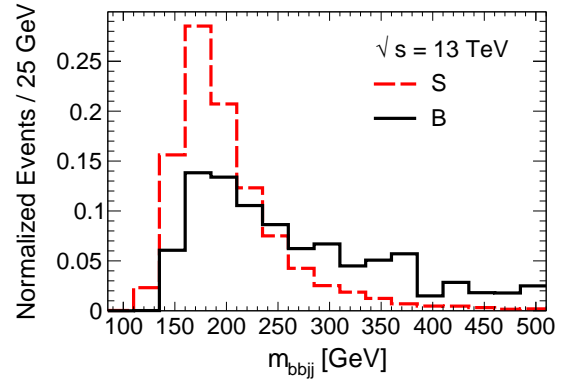


FIG. 2. m_{bbjj} distributions for the signal (red - dashed) and background (black - solid) events for the BP1.

figures include all the signal modes mentioned in Sec. II B, while the background distributions include both multi-jet and $t\bar{t}$ -jets. Clearly, the invariant masses peak at the true m_A of 70 GeV. Fig. 2 similarly shows the distributions of the $bbjj$ invariant mass for the BP1, which peaks around the true $m_{H^\pm} = 169.7$ GeV. The long tail is quite prominent in the background histogram.

Fig. 3 depicts the reconstruction of the H , as described in Sec. III C, for the BP1. The red-dashed signal histogram, corresponding to events with at least 5 b -jets, has a peak around the true $m_H = 144.7$ GeV. In this figure, the blue-dotted histogram shows the invariant mass distribution when events with 6 b -tagged jets are considered, which results in a better mass reconstruction compared to events with 5 b -jets. However, as noted earlier, estimation of the background for events with 6 b -jets is beyond the reach of our analysis.

From these histograms, we chose three bins around the true mass of each of the non-SM Higgs boson for a given BP to estimate the statistical significance, S/\sqrt{B} of its signature. For the reconstruction of the A , the S (B) implies the mean of the number of events in the bins covering m_{bb} from 45 GeV to 90 GeV for the two sig-

¹ We note here that the reconstruction efficiency for all the Higgs bosons can be further improved by imposing $\bar{\alpha} < 0.1$ and some other selection criteria noted in [53]. However, due to the large cross section of the QCD background, simulating it for such a strong selection cut would require much more substantial computational resources.

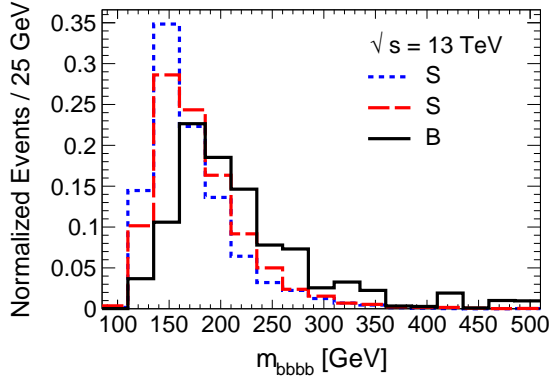


FIG. 3. m_{bbbb} distributions for the signal (red/blue - dashed) and background (black - solid) events for the BP1.

nal (background) distributions in Fig. 1. These significances are shown in Table III. The highest significance were obtained for the A – as high as 8σ in the case of the BP1 – since all the signal modes contribute to its reconstruction. For the H^\pm and H instead, the reconstruction algorithms are based on the signal topologies AAW and AAA , respectively, and other contributions therefore get reduced.

From the table, the total signal cross section after imposing the various selections cuts is considerably smaller in the case of the H compared to the H^\pm . However, the requirement of at least 5 b -tagged jets strongly suppresses the QCD background compared to the signal within the three relevant invariant mass bins for the H , which leads to a higher signal significance for it. We point out again that, for the H signal, this significance has been calculated for 5 b -tagged jets and one light jet (rather than for 6 b -jets).

For the BP2 with $m_A = 50$ GeV, we see relatively low significances for all the Higgs bosons in Table III. The invariant mass distributions corresponding to each of the reconstructed Higgs bosons for this BP can be found in the Appendix. As noted earlier, this BP was chosen so as to have almost identical m_H and m_{H^\pm} to the respective ones for the BP1, and thus to assess the impact of a reduced $\text{BR}(H \rightarrow AA)$ ($\sim 50\%$) as well as a smaller m_A on our analysis. Our reconstruction algorithm for the H is thus much more efficient when its AA is dominant by far. Furthermore, in the case of the A , the lightness of its mass results in much softer b -jets, which lowers the selection efficiency. Despite all these deficiencies, the signal significances are still a formidable $> 3\sigma$ for all the Higgs bosons for this BP, thus demonstrating the strength of our proposed reconstruction method.

V. CONCLUSIONS

In order to fully establish the EWSB dynamics triggered by the Higgs mechanism, a full reconstruction of

BP	Reconstructed Higgs boson								
	A			H^\pm			H		
	σ_S	σ_B	$\frac{S}{\sqrt{B}}$	σ_S	σ_B	$\frac{S}{\sqrt{B}}$	σ_S	σ_B	$\frac{S}{\sqrt{B}}$
1	15.5	11151.7	8σ	2.22	592.3	5σ	1.8	256.4	6.15σ
2	9.26	10369.3	5σ	1.31	460.8	3.34σ	0.8	162.2	3.43σ

TABLE III. Total signal and background cross sections (in fb) after applying all the selection cuts, and the discovery significances for the three non-SM Higgs bosons.

the Higgs potential is required. While in the SM it is relatively straightforward, in a new physics framework containing multiple Higgs fields, such as the 2HDM studied here, it would entail observing all the additional physical Higgs states and measuring their masses and couplings.

Numerous attempts, both theoretical and experimental ones, have been made to extract signatures of the two neutral Higgs bosons, besides the SM-like one, as well as the charged scalar in various Types of the 2HDM. These studies, however, generally focus on a QCD-induced single- or multiple-production, followed by a specific decay channel, of any one of these additional states, for investigating its discovery prospects at the LHC.

In some of our previous studies, we exploited the potential of the $q\bar{q}^{(\prime)}$ -initiated multi-Higgs production processes in the Type-I 2HDM and found their inclusive cross sections to be competitive with, and sometimes dominant over, QCD-induced processes. Following those, in this study we have shown, for the very first time, that all the three non-SM Higgs bosons in this model might be detectable in the unique final state with 4 (or more) b -quarks at the HL-LHC. This is possible for specific (and rather narrow) parameter space configurations, wherein intermediate pairs of relatively light Higgs bosons, produced on-shell, lead to multi- A states, which subsequently decay in the $b\bar{b}$ channel. Our sophisticated detector-level MC analysis yielded a statistical significance $> 5\sigma$ for the signals of all three non-SM Higgs state for the first of our two BPs, and in excess of 3σ for the second one.

As an outlook of our work, we advocate that, alongside the time-honoured analyses based on QCD-initiated processes, systematic investigations of the EW-induced ones are carried out as well. As our results have shown, they may prove crucial for nailing down the Type-I 2HDM as (the low-energy limit of) the new physics framework prevalent in nature.

ACKNOWLEDGMENTS

SMo is supported in part through the NExT Institute and the STFC Consolidated Grant ST/L000296/1. PS is supported by the National Research Foundation of Korea, Grant No. NRF-2022R1A2C1007583. TM's work is supported by JSPS KAKENHI Grant Number 22F21324.

APPENDIX: HISTOGRAMS FOR THE BP2

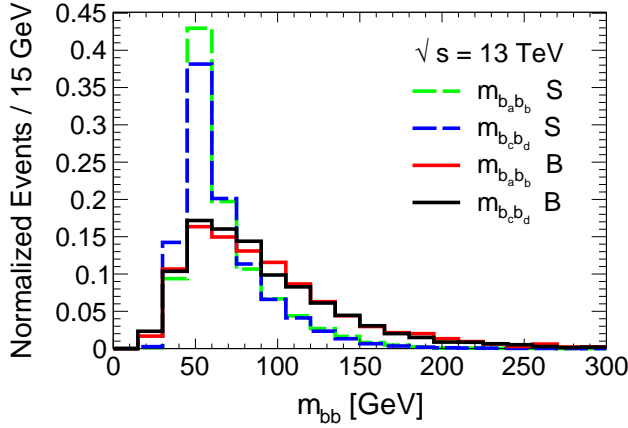


FIG. 4. Normalized bb invariant mass for the signal (green/blue - dashed) and background (black/red - solid) events.

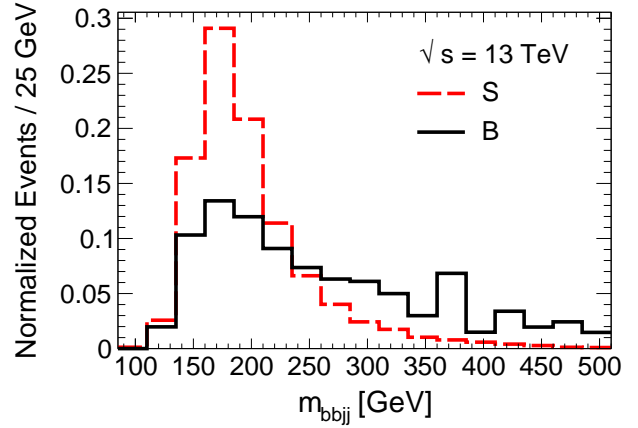


FIG. 5. Normalized $bbjj$ invariant mass for the signal (red - dashed) and background (black - solid) events.

[1] Georges Aad *et al.* (ATLAS), “Observation of a new particle in the search for the Standard Model Higgs boson with the ATLAS detector at the LHC,” *Phys. Lett. B* **716**, 1–29 (2012), [arXiv:1207.7214 \[hep-ex\]](#).

[2] Serguei Chatrchyan *et al.* (CMS), “Observation of a new boson at a mass of 125 GeV with the CMS experiment at the LHC,” *Phys. Lett. B* **716**, 30–61 (2012), [arXiv:1207.7235 \[hep-ex\]](#).

[3] Sheldon L. Glashow and Steven Weinberg, “Natural Conservation Laws for Neutral Currents,” *Phys. Rev. D* **15**, 1958 (1977).

[4] E. A. Paschos, “Diagonal Neutral Currents,” *Phys. Rev. D* **15**, 1966 (1977).

[5] John F. Gunion, Howard E. Haber, Gordon L. Kane, and Sally Dawson, “The Higgs Hunter’s Guide,” *Front. Phys.* **80**, 1–404 (2000).

[6] G.C. Branco, P.M. Ferreira, L. Lavoura, M.N. Rebelo, Marc Sher, *et al.*, “Theory and phenomenology of two-Higgs-doublet models,” *Phys. Rept.* **516**, 1–102 (2012), [arXiv:1106.0034 \[hep-ph\]](#).

[7] Abdesslam Arhrib, Rachid Benbrik, Chuan-Hung Chen, Renato Guedes, and Rui Santos, “Double Neutral Higgs production in the Two-Higgs doublet model at the LHC,” *JHEP* **08**, 035 (2009), [arXiv:0906.0387 \[hep-ph\]](#).

[8] Benoit Hespel, David Lopez-Val, and Eleni Vryonidou, “Higgs pair production via gluon fusion in the Two-Higgs-Doublet Model,” *JHEP* **09**, 124 (2014), [arXiv:1407.0281 \[hep-ph\]](#).

[9] Rikard Enberg, William Klemm, Stefano Moretti, and Shoaib Munir, “Electroweak production of light scalar–pseudoscalar pairs from extended Higgs sectors,” *Phys. Lett. B* **764**, 121–125 (2017), [arXiv:1605.02498 \[hep-ph\]](#).

[10] Abdesslam Arhrib, Rachid Benbrik, and Stefano

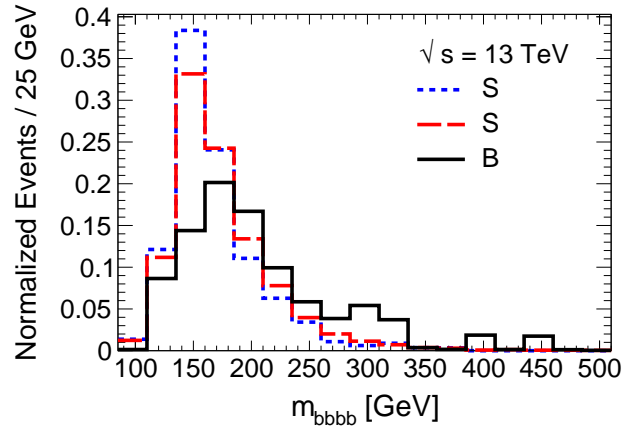


FIG. 6. Normalized $bbbb$ invariant mass for the signal (red/blue - dashed) and background (black - solid).

Moretti, “Bosonic Decays of Charged Higgs Bosons in a 2HDM Type-I,” *Eur. Phys. J. C* **77**, 621 (2017), [arXiv:1607.02402 \[hep-ph\]](#).

[11] Abdesslam Arhrib, Rachid Benbrik, Stefano Moretti, Abdessamad Rouchad, Qi-Shu Yan, and Xianhui Zhang, “Multi-photon production in the Type-I 2HDM,” (2017), [arXiv:1712.05332 \[hep-ph\]](#).

[12] Abdesslam Arhrib, Rachid Benbrik, Rikard Enberg, William Klemm, Stefano Moretti, and Shoaib Munir, “Identifying a light charged Higgs boson at the LHC Run II,” *Phys. Lett. B* **774**, 591–598 (2017), [arXiv:1706.01964 \[hep-ph\]](#).

[13] Wenhai Xie, R. Benbrik, Abdeljalil Habjia, Souad Taj,

- Bin Gong, and Qi-Shu Yan, “Signature of 2HDM at Higgs Factories,” *Phys. Rev. D* **103**, 095030 (2021), [arXiv:1812.02597 \[hep-ph\]](#).
- [14] Abdesslam Arhrib, Rachid Benbrik, Hicham Harouiz, Stefano Moretti, Yan Wang, and Qi-Shu Yan, “Implications of a light charged Higgs boson at the LHC run III in the 2HDM,” *Phys. Rev. D* **102**, 115040 (2020), [arXiv:2003.11108 \[hep-ph\]](#).
- [15] A. Arhrib, R. Benbrik, M. Krab, B. Manaut, S. Moretti, Yan Wang, and Qi-Shu Yan, “New discovery modes for a light charged Higgs boson at the LHC,” *JHEP* **10**, 073 (2021), [arXiv:2106.13656 \[hep-ph\]](#).
- [16] Yan Wang, A. Arhrib, R. Benbrik, M. Krab, B. Manaut, S. Moretti, and Qi-Shu Yan, “Analysis of $W + 4\gamma$ in the 2HDM Type-I at the LHC,” *JHEP* **12**, 021 (2021), [arXiv:2107.01451 \[hep-ph\]](#).
- [17] Oliver Atkinson, Matthew Black, Alexander Lenz, Aleksey Rusov, and James Wynne, “Cornering the Two Higgs Doublet Model Type II,” *JHEP* **04**, 172 (2022), [arXiv:2107.05650 \[hep-ph\]](#).
- [18] Tanmoy Mondal and Prasenjit Sanyal, “Same sign trilepton as signature of charged Higgs in two Higgs doublet model,” *JHEP* **05**, 040 (2022), [arXiv:2109.05682 \[hep-ph\]](#).
- [19] Shinya Kanemura, Michihisa Takeuchi, and Kei Yagyu, “Probing double-aligned two-Higgs-doublet models at the LHC,” *Phys. Rev. D* **105**, 115001 (2022), [arXiv:2112.13679 \[hep-ph\]](#).
- [20] M. Krab, M. Ouchemhou, A. Arhrib, R. Benbrik, B. Manaut, and Qi-Shu Yan, “Single charged Higgs boson production at the LHC,” *Phys. Lett. B* **839**, 137705 (2023), [arXiv:2210.09416 \[hep-ph\]](#).
- [21] Kingman Cheung, Adil Jueid, Jinheung Kim, Soojin Lee, Chih-Ting Lu, and Jeonghyeon Song, “Comprehensive study of the light charged Higgs boson in the type-I two-Higgs-doublet model,” *Phys. Rev. D* **105**, 095044 (2022), [arXiv:2201.06890 \[hep-ph\]](#).
- [22] Jinheung Kim, Soojin Lee, Jeonghyeon Song, and Prasenjit Sanyal, “Fermiophobic light Higgs boson in the type-I two-Higgs-doublet model,” *Phys. Lett. B* **834**, 137406 (2022), [arXiv:2207.05104 \[hep-ph\]](#).
- [23] Jinheung Kim, Soojin Lee, Prasenjit Sanyal, Jeonghyeon Song, and Daohan Wang, “ $\tau^\pm\nu\gamma\gamma$ and $\ell^\pm\ell^\pm\gamma\gamma E_T X$ to probe the fermiophobic Higgs boson with high cutoff scales,” (2023), [arXiv:2302.05467 \[hep-ph\]](#).
- [24] Yi-Lun Chung, Kingman Cheung, and Shih-Chieh Hsu, “Sensitivity of two-Higgs-doublet models on Higgs-pair production via bb^-bb^- final state,” *Phys. Rev. D* **106**, 095015 (2022), [arXiv:2207.09602 \[hep-ph\]](#).
- [25] Anna Ivina (ATLAS), “Search for light charged Higgs boson in $t \rightarrow H^\pm + b(H^\pm \rightarrow cb)$ decays with the ATLAS detector at LHC,” *PoS EPS-HEP2021*, 631 (2022).
- [26] “Search for heavy resonances decaying into a Z or W boson and a Higgs boson in final states with leptons and b -jets in 139 fb^{-1} of pp collisions at $\sqrt{s} = 13 \text{ TeV}$ with the ATLAS detector,” (2022), [arXiv:2207.00230 \[hep-ex\]](#).
- [27] “Search for displaced photons produced in exotic decays of the Higgs boson using 13 TeV pp collisions with the ATLAS detector,” (2022), [arXiv:2209.01029 \[hep-ex\]](#).
- [28] “A search for heavy Higgs bosons decaying into vector bosons in same-sign two-lepton final states in pp collisions at $\sqrt{s} = 13 \text{ TeV}$ with the ATLAS detector,” (2022), [arXiv:2211.02617 \[hep-ex\]](#).
- [29] Armen Tumasyan *et al.* (CMS), “Search for new particles in an extended Higgs sector with four b quarks in the final state at $s=13\text{TeV}$,” *Phys. Lett. B* **835**, 137566 (2022), [arXiv:2203.00480 \[hep-ex\]](#).
- [30] “Search for a massive scalar resonance decaying to a light scalar and a Higgs boson in the four b quarks final state with boosted topology,” (2022), [arXiv:2204.12413 \[hep-ex\]](#).
- [31] “Search for a charged Higgs boson decaying into a heavy neutral Higgs boson and a W boson in proton-proton collisions at $\sqrt{s} = 13 \text{ TeV}$,” (2022), [arXiv:2207.01046 \[hep-ex\]](#).
- [32] “Search for the exotic decay of the Higgs boson into two light pseudoscalars with four photons in the final state in proton-proton collisions at $\sqrt{s} = 13 \text{ TeV}$,” (2022), [arXiv:2208.01469 \[hep-ex\]](#).
- [33] Rikard Enberg, William Klemm, Stefano Moretti, and Shoaib Munir, “Electroweak production of multiple (pseudo)scalars in the 2HDM,” *Eur. Phys. J. C* **79**, 512 (2019), [arXiv:1812.01147 \[hep-ph\]](#).
- [34] Farvah Mahmoudi, “Overview of the interpretation of indirect searches for charged Higgs bosons in the 2HDM,” *Proceedings, 6th International Workshop on Prospects for Charged Higgs Discovery at Colliders (CHARGED 2016): Uppsala, Sweden, October 3-6, 2016*, *PoS CHARGED2016*, 012 (2017).
- [35] Jérémy Bernon, John F. Gunion, Howard E. Haber, Yun Jiang, and Sabine Kraml, “Scrutinizing the alignment limit in two-Higgs-doublet models. II. $m_H=125??\text{GeV}$,” *Phys. Rev. D* **93**, 035027 (2016), [arXiv:1511.03682 \[hep-ph\]](#).
- [36] David Eriksson, Johan Rathsman, and Oscar Stal, “2HDMC: Two-Higgs-Doublet Model Calculator Physics and Manual,” *Comput. Phys. Commun.* **181**, 189–205 (2010), [arXiv:0902.0851 \[hep-ph\]](#).
- [37] R. L. Workman *et al.* (Particle Data Group), “Review of Particle Physics,” *PTEP* **2022**, 083C01 (2022).
- [38] F. Mahmoudi, “SuperIso v2.3: A Program for calculating flavor physics observables in Supersymmetry,” *Comput. Phys. Commun.* **180**, 1579–1613 (2009), [arXiv:0808.3144 \[hep-ph\]](#).
- [39] Prasenjit Sanyal, “Limits on the Charged Higgs Parameters in the Two Higgs Doublet Model using CMS $\sqrt{s} = 13 \text{ TeV}$ Results,” *Eur. Phys. J. C* **79**, 913 (2019), [arXiv:1906.02520 \[hep-ph\]](#).
- [40] Philip Bechtle, Oliver Brein, Sven Heinemeyer, Oscar Stål, Tim Stefaniak, *et al.*, “HiggsBounds – 4: Improved Tests of Extended Higgs Sectors against Exclusion Bounds from LEP, the Tevatron and the LHC,” *Eur. Phys. J. C* **74**, 2693 (2014), [arXiv:1311.0055 \[hep-ph\]](#).
- [41] Jonathon Mark Langford (ATLAS, CMS), “Combination of Higgs measurements from ATLAS and CMS : couplings and $||$ - framework,” *PoS LHCP2020*, 136 (2021).
- [42] Richard D. Ball *et al.* (NNPDF), “Parton distributions from high-precision collider data,” *Eur. Phys. J. C* **77**, 663 (2017), [arXiv:1706.00428 \[hep-ph\]](#).
- [43] Michal Czakon and Alexander Mitov, “Top++: A Program for the Calculation of the Top-Pair Cross-Section at Hadron Colliders,” *Comput. Phys. Commun.* **185**,

- 2930 (2014), [arXiv:1112.5675 \[hep-ph\]](#).
- [44] Henning Bahl, Tim Stefaniak, and Jonas Wittbrodt, “The forgotten channels: charged Higgs boson decays to a W and a non-SM-like Higgs boson,” *JHEP* **06**, 183 (2021), [arXiv:2103.07484 \[hep-ph\]](#).
- [45] Johan Alwall, Michel Herquet, Fabio Maltoni, Olivier Mattelaer, and Tim Stelzer, “MadGraph 5 : Going Beyond,” *JHEP* **06**, 128 (2011), [arXiv:1106.0522 \[hep-ph\]](#).
- [46] J. Alwall, R. Frederix, S. Frixione, V. Hirschi, F. Maltoni, O. Mattelaer, H. S. Shao, T. Stelzer, P. Torrielli, and M. Zaro, “The automated computation of tree-level and next-to-leading order differential cross sections, and their matching to parton shower simulations,” *JHEP* **07**, 079 (2014), [arXiv:1405.0301 \[hep-ph\]](#).
- [47] Torbjorn Sjostrand, Stephen Mrenna, and Peter Z. Skands, “PYTHIA 6.4 Physics and Manual,” *JHEP* **05**, 026 (2006), [arXiv:hep-ph/0603175](#).
- [48] Torbjörn Sjöstrand, Stefan Ask, Jesper R. Christiansen, Richard Corke, Nishita Desai, Philip Ilten, Stephen Mrenna, Stefan Prestel, Christine O. Rasmussen, and Peter Z. Skands, “An Introduction to PYTHIA 8.2,” *Comput. Phys. Commun.* **191**, 159–177 (2015), [arXiv:1410.3012 \[hep-ph\]](#).
- [49] Matteo Cacciari, Gavin P. Salam, and Gregory Soyez, “The Anti-k(t) jet clustering algorithm,” *JHEP* **04**, 063 (2008), [arXiv:0802.1189 \[hep-ph\]](#).
- [50] Serguei Chatrchyan *et al.* (CMS), “Identification of b-Quark Jets with the CMS Experiment,” *JINST* **8**, P04013 (2013), [arXiv:1211.4462 \[hep-ex\]](#).
- [51] J. de Favereau, C. Delaere, P. Demin, A. Giammanco, V. Lemaitre, A. Mertens, and M. Selvaggi (DELPHES 3), “DELPHES 3, A modular framework for fast simulation of a generic collider experiment,” *JHEP* **02**, 057 (2014), [arXiv:1307.6346 \[hep-ex\]](#).
- [52] R. Brun and F. Rademakers, “ROOT: An object oriented data analysis framework,” *Nucl. Instrum. Meth. A* **389**, 81–86 (1997).
- [53] “Search for resonant and nonresonant production of pairs of dijet resonances in proton-proton collisions at $\sqrt{s} = 13$ TeV”, Tech. Rep. (CERN, Geneva, 2022), [arXiv:2206.09997 \[hep-ex\]](#).